Theoretical Study of the Photodissociation and Hydrogenation of the Fluorene Cation

Jan Szczepanski, Mark J. Dibben, Wright Pearson, John R. Eyler,* and Martin Vala*

Department of Chemistry and Center for Chemical Physics, University of Florida, Gainesville, Florida 32611-7200

Received: May 15, 2001; In Final Form: August 17, 2001

Previous Fourier transform ion cyclotron resonance mass spectrometry (FTICR/MS) experiments have shown that UV/visible photolysis of the fluorene cation leads primarily to sequential loss of one to five hydrogens. Subsequent photolysis of the odd mass dehydrogenated species induces further fragmentation to lower mass products. In the present paper, results from density functional calculations are used to explain the experimental findings. These results show that dehydrogenation is predicted to occur first from the sp^3 carbon on the five-membered ring and then from only one of the six-membered rings. The predicted infrared spectrum of this $C_{13}H_5^+$ (*m*/*z* 161) species is shown to match well with a matrix isolation spectrum of a photolyzed fluorene sample. The conclusion is drawn that the $C_{13}H_5^+$ (*m*/*z* 161) ion retains its fluorene-like framework and does not isomerize upon dehydrogenation. Photolysis of this $C_{13}H_5^+$ (*m*/*z* 161) ion does appear to lead to isomerization. Plausible photodecomposition pathways leading from this (and other) species to the observed low-mass products are shown to be possible only if it is assumed that the fluorene framework opens to a monocyclic ring. Unusual geometries, such as a "tadpole" shape (three-membered ring attached to a linear carbon chain) for the $C_5H_3^+$ species, a three-membered ring fused to a six-membered ring for the $C_7H_5^+$ product and monocyclic rings for the all-carbon C_9^+ and C_{11}^+ product ions are computed to be the most stable for these observed products.

I. Introduction

Interest in polycyclic aromatic hydrocarbons (PAHs) has remained strong for many years because of the involvement of these species in combustion[1] and astrophysical processes.[2−7] There has also been considerable interest in PAHs because of the suggestion that they may undergo photoinduced rearrangements or isomerizations prior to fragmentation.

Ekern and co-workers reported the complete dehydrogenation of the coronene cation ($C_{24}H_{12}^+$) and the naphthopyrene cation ($C_{24}H_{14}^+$) after brief UV/visible photolysis.[8] This finding naturally led to speculation about the structural form of the C_{24}^+ moiety and to questions of possible isomerization to monocyclic ring, linear chain or fullerene type structures. No definitive answer has yet been offered.

Later, Ekern et al. reported that UV/visible photolysis causes the fluorene cation to lose up to five hydrogens.[9] Other PAH cations were found to behave differently under similar photolysis conditions. In a very recent study, the photolysis of fluorene cations (*m*/*z* 166) was studied in greater detail.[10] Single hydrogen loss was found to occur sequentially. Dual hydrogen loss occurred as a minor decomposition pathway only from odd mass precursors (*m*/*z* 163 and 165). Further irradiation of the dehydrogenated species resulted in fragmentation to lower mass species. Rate constants and branching ratios of these decomposition pathways were determined.

In the present paper, results of theoretical calculations on the photodecomposition of the fluorene cation are presented. It is shown that density functional theory calculations can be used to determine energetically plausible photofragmentation pathways that explain the observed decomposition products. In addition, the computed infrared absorption spectra for the fluorene cation and several of its dehydrogenated partners are also reported.

II. Computational Procedures

Geometries were optimized and harmonic frequencies calculated using hybrid density functional theory (B3LYP method) with either 4-31G or 6-31G(d,p) basis sets using the Gaussian 98 platform.[11] The B3LYP/4-31G level of theory was used for most bond energy calculations. Bauschlicher has shown that this approach is relatively accurate in predicting H−H and C−H bond energies in H_2 and C_6H_6, respectively.[12] Use of the 6-31G(d,p) basis set results in only small improvements in the computed harmonic frequencies (scaled) for neutral and cationic fluorene when compared to matrix band frequencies. Following common practice, we have used the same scaling factor to correct both zero-point energies (ZPE) and harmonic frequencies. All calculated energies have been ZPE-corrected by a factor of either 0.957 (4-31G) or 0.978 (6-31G(d,p)). This factor brings the calculated harmonic frequencies of the fluorene cation in line with experimental (Ar matrix) band positions (minimum error deviation) for the 600−1150 cm^{-1} energy region. Langhof introduced a similar scaling factor (0.978) in his successful comparison of calculated (B3LYP/4-31G) and experimental (Ar matrix) band frequencies for a large group of PAH cations.[13] Bauschlicher has also recommended the use of the B3LYP/4-31G level of theory for the calculation of C−H bond energies in relatively large systems, such as PAH cations.[12] The bond energies for H_2 and C_6H_6 (C−H) computed using 4-31G (6-31G(d,p)) basis sets are 103.7 kcal/mol (105.5 kcal/mol) and 110.7 kcal/mol (110.4 kcal/mol), respectively. The corresponding experimental bond energies are 103.3 and 109.8/109.4 kcal/

* Corresponding author. E-mail: mvala@chem.ufl.edu.

10.1021/jp011870l CCC: $20.00 © 2001 American Chemical Society
Published on Web 09/25/2001

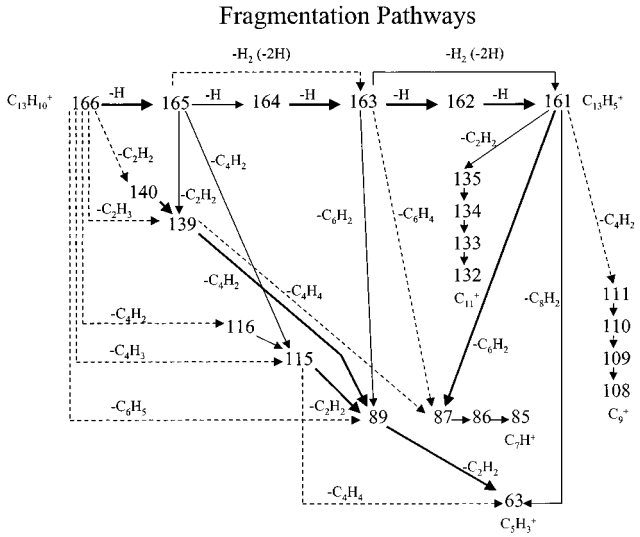

Figure 1. Photofragmentation reaction pathways observed in the FTICR mass spectrometric study of the fluorene cation, $C_{13}H_{10}^+$ (*m*/*z* 166), isolated in a 2 T ICR for a photon flux of ca. 3×10^{13} photons s^{-1} cm^{-2} nm^{-1} (at 360 nm) from a Xe lamp (1−4 s exposure). Specific reaction pathways were tracked by isolation of the lower mass fragment and observation of product ions after photolysis. Adapted from ref 10.

mol.[12] Thus, our choice of the 4-31G basis is justified from the point of view of accuracy and cost. Over 150 molecular systems, each with between 8 and 25 atoms, were calculated in the present work.

III. Results and Discussion

a. Sequential Hydrogen Loss. The primary photodissociation route for the fluorene cation is the sequential loss of five hydrogens.[9,10] Figure 1 shows the experimentally determined photodecomposition pathways and products, and emphasizes that the primary route is the loss of hydrogen atoms. The most probable positions from which these hydrogens are lost were first determined.

i. Loss of First Hydrogen. The position of the first hydrogen loss was calculated by finding the C−H bond energies at all H positions on the fluorene framework by determining the total energy of the $C_{13}H_{10}^+$ ion and subtracting this value from the total energy of the H + $C_{13}H_9^+$ products. The C−H bond energies are listed in Table 1. Figure 2 shows the energetically favorable calculated photoreaction pathways for sequential hydrogen loss. The C−H bonds (C−H9 and C−H9′) on the five-membered ring are almost 50% weaker than the C−H bonds on the six-membered rings. This bond energy (2.64 eV (60.9 kcal/mol)) is similar to the value found by Bauschlicher for hydrogens bonded to the same carbon in the 1-hydronaphthalene cation (62.1 kcal/mol).[12]

Computation of the transition state (TS) involved in the abstraction of the H9′ atom revealed no barrier before the dissociation limit of the C−H9′ bond. This is not surprising since the optimized geometry of the TS shows that the H9′ atom is 3.26 Å from the sp^3 carbon and 2.12 Å from the H9 atom, indicating that H9′ interacts only minimally with the rest of the ion. This situation is similar to the abstraction of the hydrogen from the 1-position of the 1-hydronaphthalene cation, where a zero energy barrier was also found.[12]

ii. Loss of Second Hydrogen. The most favorable route for the loss of the next hydrogen from $C_{13}H_9^+$ ($C_{13}H_{10}^+$ with H9′ removed) is the cleavage of the C−H6 (or equivalent C−H3) bond. This requires 4.88 eV. However, this energy is only ca. 3% lower than cleavage of the C−H9 bond, suggesting that this reaction channel (i.e., *m*/*z* 165 − H6 = 164a in Table 1) is only slightly more favorable than the channels in which the other hydrogens are removed.

iii. Loss of Third Hydrogen. In the loss of the third hydrogen, the C−H bond energies at the H5−H8 (or equivalent H1−H4) positions in the $C_{13}H_8^+$ ion (created from $C_{13}H_{10}^+$ by H9′ and

TABLE 1: C−H Bond Energies (eV) Calculated at B3LYP/4-31G and B3LYP/6-31G(d,p) (in Parentheses) Levels of Theory for Sequential Hydrogen Loss in Photodissociation Reactions of the Fluorene Cation ($C_{13}H_{10}^+$, *m*/*z* 166)[a]

	H removed									
precursor label	H1	H2	H3	H4	H5	H6	H7	H8	H9	H9′
				First H Loss (*m*/*z*166 → 165)						
(166)	5.01 (4.92)	5.23 (5.13)	5.10	5.04	5.04	5.10	5.23 (5.13)	5.01 (4.92)	**2.64 (2.69)**	**2.64 (2.69)**
				Second H Loss (*m*/*z*165 → 164)						
H9′ off (165)	**4.90**	**4.95**	**4.88 (4.86)**	**4.91 (4.89)**	**4.91 (4.89)**	**4.88 (4.86)**	**4.95**	**4.90**	**5.03**	
				Third H Loss (*m*/*z* 164 → 163)						
H9′, H5 off (164b)	6.87	6.95	6.42[b]	6.96 (6.26)[b]		**3.96 (3.94)**	5.04	**4.25**	5.43	
H9′, H6 off (164a)	6.52[b]	7.02	6.95	6.44[b]	**3.98**		**4.01**	4.49	6.52	
H9′, H7 off (164d)	6.84	6.93	6.96	6.91	5.00	**3.94**		**3.96**	6.32	
H9′, H8 off (164c)	6.67[b]	6.89	6.50[b]	6.89	**4.25**	4.47	**4.00**		5.80	
H9′, H9 off	5.67	6.23	6.37	5.22	5.22	6.37	6.23	5.67		
				Fourth H Loss (*m*/*z* 163 → 162)						
H9′, H5, H6 off (163b)	4.91	4.95	4.90	4.94			**4.71**	**4.87**	4.98	
H9′, H5, H8 off (163c)	5.46	4.93	5.46	5.47		**4.57**	**4.64**		5.48	
H9′, H6, H7 off (163a)	4.91	4.95	4.89	4.91	**4.68**			**4.64**	5.05	
H9′, H7, H8 off (163d)	4.91	4.96	4.90	4.91	**4.89**	**4.63**			5.07	
				Fifth H Loss (*m*/*z*162 → 161)						
H9′, H5, H6, H7 off (162a)	6.65	6.72	6.54	6.79				**4.28**	5.50	
H9′, H5, H6, H8 off (162b)	6.49[b]	6.51[b]	6.37[b]	6.43[b]			**4.13**		6.39[b]	
H9′, H5, H8, H7 off (162c)	6.45[b]	6.82	6.36[b]	6.63[b]		**4.06 (4.11)**			**3.27 (3.63)**	
H9′, H6, H7, H8 off (162d)	6.38[b]	6.67[b]	6.48[b]	6.45[b]	**4.33**				5.86	
				Sixth H Loss (*m*/*z*161 → 160)						
H9′, H5, H6, H7, H8 off (161)	4.90	4.93	4.89	4.92					4.99	
H9′, H5, H8, H7, H9 off	6.70	6.70	6.63	6.54		5.79				

[a] Energies are ZPE-corrected (× 0.957(4-31G) or × 0.978 (6-31G(d,p)). Hydrogen and precursor labeling is defined in Figure 2. Energetically favorable reactions are given in bold type. [b] One imaginary frequency was found for the calculated product.

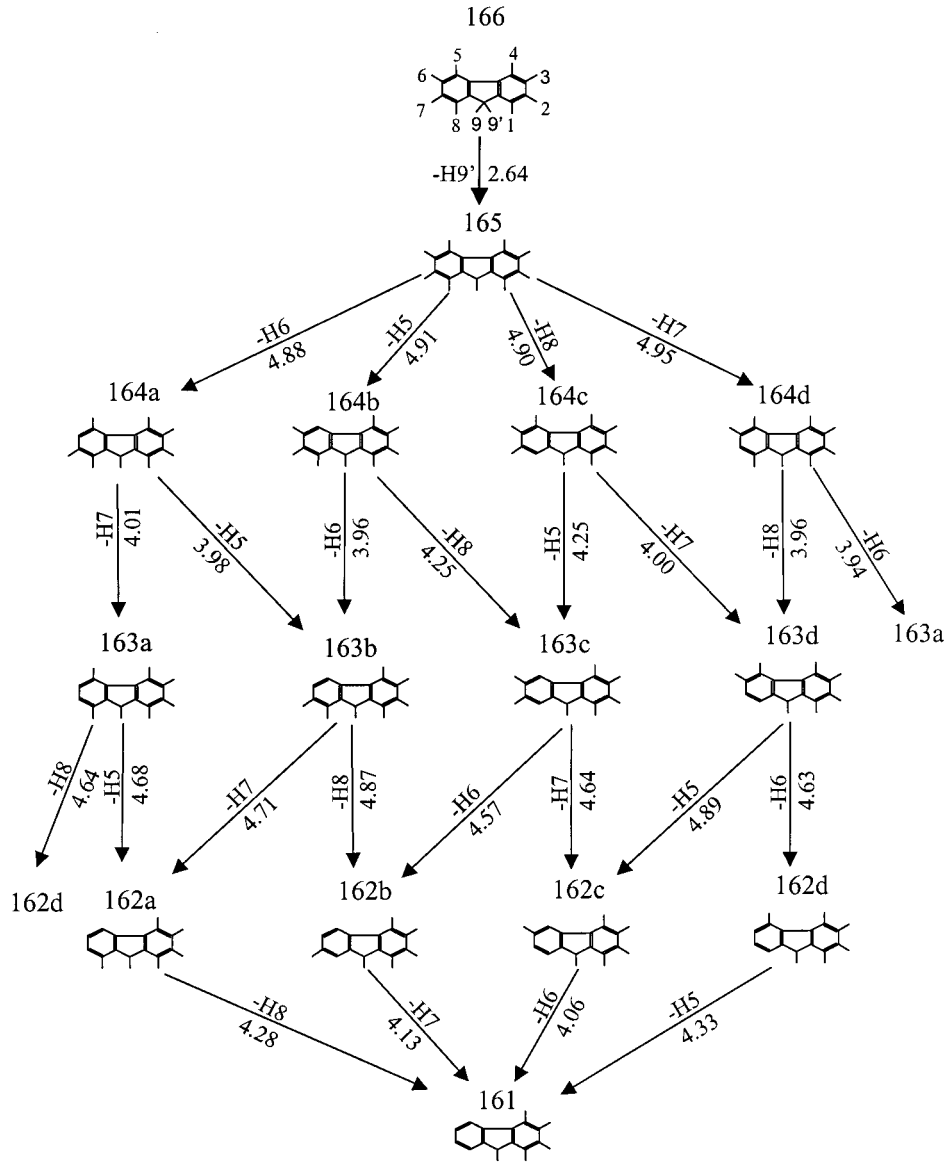

Figure 2. Calculated (B3LYP/4-31G) energetically favorable photoreaction pathways for sequential hydrogen loss (up to five hydrogens) from the fluorene cation ($C_{13}H_{10}^+$, *m*/*z* 166). The C−H bond energies (in eV, ZPE × 0.957 scale factor) for particular hydrogen losses are indicated. The hydrogen losses shown represent possible routes for the *m*/*z* 166 → 161 dissociation shown in Figure 1.

H9 atom loss) require from 5.22 to 6.37 eV (cf. Table 1). These energies are ca. 30 and 59% higher, respectively, than the bond energies in the preferred, bold-typed reactions, indicating their probable low yield. (They are therefore not displayed in Figure 2.)

Abstraction of H8 from form 164a, H7 from 164b, H6 from 164c and H5 from 164d requires 4.5, 5.04, 4.5, and 5.0 eV energy, respectively. These energies are significantly larger than those displayed for the third H loss in Figure 2. They are expected to be low-yield routes. Finally, removal of the third hydrogen from the *same* six-membered ring requires lower energies than removal from the *other* six-membered ring. Removing hydrogen from the same ring requires 3.94−4.25 eV, while stripping from the other ring requires 50−75% more energy (cf. Table 1).

Consequently, in the third H loss step, only four forms (a−d) of the *m*/*z* 164 precursor were studied. Figure 2 shows eight energetically plausible reaction pathways starting from these four precursors. C−H bond energies range from 3.94 to 4.25 eV. Table 1 lists the energies of all the reactions involving these four *m*/*z* 164 fluorene-like isomeric precursors.

iv. Loss of Fourth Hydrogen. Eight routes are possible for the loss of the fourth hydrogen. In this as well as in the second H loss step, the precursors are in their singlet ground states. The computed C−H bond energies are higher by 15−24% than the energies in the third and fifth H loss step, where the precursors are in doublet ground states. Again, abstraction of the fourth H from the *other* six-membered ring (i.e., H1−H4), or the abstraction of H9, requires higher energies (between 6 and 9.3% more) than removing H5−H8 via the reactions displayed in Figure 2.

v. Loss of Fifth Hydrogen. Five reaction channels from four different $C_{13}H_6^+$ isomers are favored for the removal of the fifth hydrogen (cf. Table 1). The removal of H from one of the rings of the ion requires 4.06−4.33 eV. Removal of the fifth hydrogen from the *other* six-membered ring requires 35−47% more energy and is therefore much less likely. Removing H9 from the 162c precursor requires only 3.27 eV. This creates a second *m*/*z*161 isomeric fragment (the first is displayed in Figure 2). The *m*/*z* 161 isomer of Figure 2 is formed in four reactions, while the second one is only formed in one reaction. Therefore, the former isomer is expected be in much higher abundance.

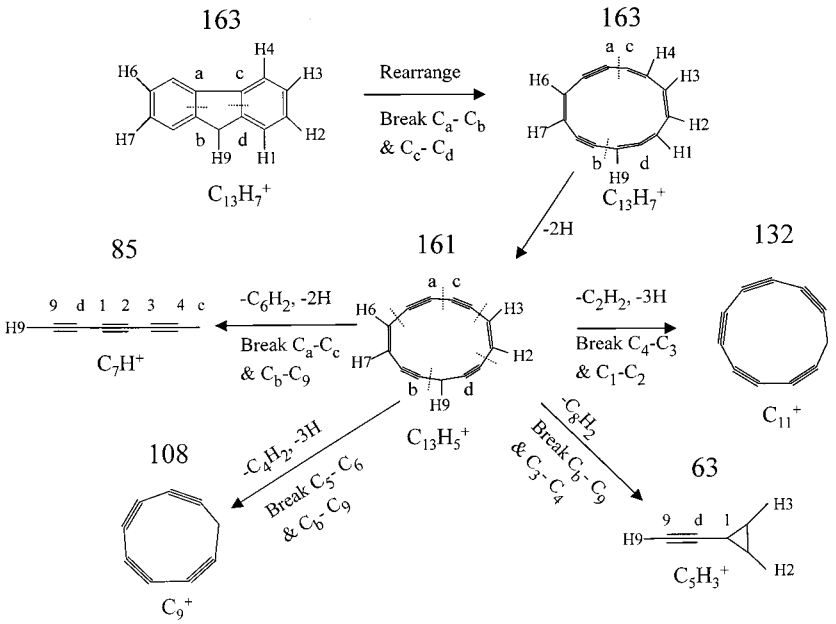

Figure 3. Formation of cyclic *m*/*z* 163 ($C_{13}H_7^+$) and *m*/*z* 161 ($C_{13}H_5^+$) ions by rupture of the C_a-C_b and C_c-C_d bonds in the proposed ring-opening mechanism. The final lowest energy photoproducts are formed via the opening of the specific bonds marked.

vi. Improbable Loss of Sixth Hydrogen. The observed loss of only five hydrogens is understandable now, since the C−H bond energies calculated for the *m*/*z* 161 ($C_{13}H_5^+$) species (sixth H loss in Table 1) are high (over 4.89 eV). On the other hand, other photoproducts are observed that originate from the *m*/*z* 161 species. These decomposition pathways, involving loss of neutral C_2H_2, C_4H_2, C_6H_2, and C_8H_2 species, are energetically more favorable than loss of another hydrogen. These products are discussed in the next section.

We have used the 6-31G(d,p) basis set for several C−H bond energy calculations. For the reactions involving the loss of only one H from the fluorene cation, only small differences are observed in bond energies compared with the results using the 4-31G basis set (cf. Table 1). The B3LYP/6-31(d,p) C−H bond energies do not change the order of reactions in Figure 2. However, use of the more reliable (but many times more costly) electron correlation methods for C−H bond energy calculations could reorder the reactions in Table 1.

In summary, the B3LYP/4-31G bond energies listed in Table 1 and Figure 2 indicate that the first hydrogen removed from the fluorene cation is from the sp^3 carbon on the five-membered ring, and the next four hydrogens come from one of the six-membered rings. Loss of the sixth hydrogen is not energetically feasible under the photolysis conditions used in the experiment.

b. Structural Integrity vs Ring Opening. Further photolysis of the dehydrogenated odd mass fluorene species (*m*/*z* 161, 163, 165) has been observed to produce a number of low-mass fragments.[10]

These low-mass products *cannot* be understood satisfactorily starting from a fluorene-like framework. However, production of all the product fragments can be explained in a consistent and plausible manner if one or more rings are assumed to open and C_2H_2, C_2H_4, and/or C_2H_6 fragments are ejected.

In our initial calculations, the *m*/*z* 165 precursor was assumed to retain its fluorene-like carbon framework. Then the C_a-C_b bond in the $C_{13}H_9^+$ ion was broken and the C_a-C_b distance increased stepwise. (Of the C−C bonds in the fluorene cation framework, the C_a-C_b and C_c-C_d internal bonds (for labels, cf. Figure 3) are the weakest (and among the longest).) Single point total energy calculations were performed (B3LYP/4-31G) on the singlet potential surface for each step. A plot of total energy vs *R* (C_a-C_b) distances showed a local *maximum*, but at greater distances the total energies decreased, indicating that $C_{13}H_9^+$ forms other, more stable structures that are not fluorene-like in structure. However, these calculated energies are not expected to be completely reliable, since the geometries were not first optimized. Calculations (B3LYP/4-31G) on energetically relaxed cyclic structures with the C_a-C_b and C_c-C_d bonds open for the $C_{13}H_9^+$, $C_{13}H_7^+$, and $C_{13}H_5^+$ ions yielded total energies of +6.23, +2.59, and −0.33 eV, respectively, relative to the closed-bond fluorene forms. This suggests that ring opening may occur in the $C_{13}H_7^+$ and $C_{13}H_5^+$ singlet state ions when exposed to radiation with energies up to 5.5 eV (as used in the previous experiments).[10] On the other hand, formation of monocyclic $C_{13}H_5^+$ may also occur by the loss of two hydrogens from cyclic $C_{13}H_7^+$ (cf. Figure 3). Thus, it appears possible that both fluorene-like *and* cyclic isomers of $C_{13}H_7^+$ and $C_{13}H_5^+$ could be generated in the FTICR/MS experiments.

c. Further Fragmentation. Although our earlier study[9] with short photolysis exposures found only dehydrogenated products, later work[10] determined that longer irradiation times lead to other, lower mass products. Isolation and further photolysis of each of the dehydrogenated product ions results in a set of unique lower mass products, as shown in Figure 1. To rationalize the formation of these products, the strategy adopted was to establish the lowest energy C−C bond-cleavage route that leads to the observed low-mass products without requiring repositioning of any hydrogen atoms. The possible pathways from each of the odd mass dehydrogenated precursors are discussed in turn below.

i. Photoproducts from the m/z 165 Ion. Photolysis of the *m*/*z* 165 ion yields *m*/*z* 164, 163, 139, and 115 product ions directly (cf. Figure 1). Breaking a pair of C−C bonds in the $C_{13}H_9^+$ species with ejection of C_2H_2 and C_4H_2 neutral fragments could lead to the observed *m*/*z* 139 ($C_{11}H_7^+$) and *m*/*z* 115 ($C_9H_7^+$) ions, respectively. Further ejection of two C_2H_2 fragments from the *m*/*z* 115 ion could lead ultimately to the $C_5H_3^+$ (*m*/*z* 63) ion. However, the *m*/*z* 63 ion could also be formed from the *m*/*z* 139 ion by ejection of C_2H_2 and C_4H_2 fragments (cf. Figure 1). Isolation of the *m*/*z* 139 ion followed by further photolysis

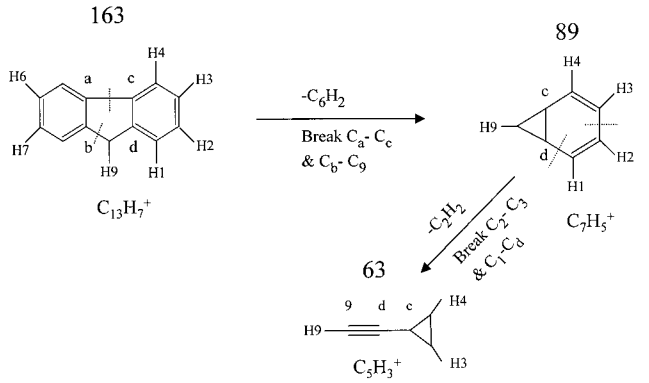

Figure 4. Formation of *m*/*z* 89 ($C_7H_5^+$) ions directly from *m*/*z* 163 isomer ($C_{13}H_7^+$ form c in Figure 2). Note that no hydrogen migrations are necessary in these reaction pathways.

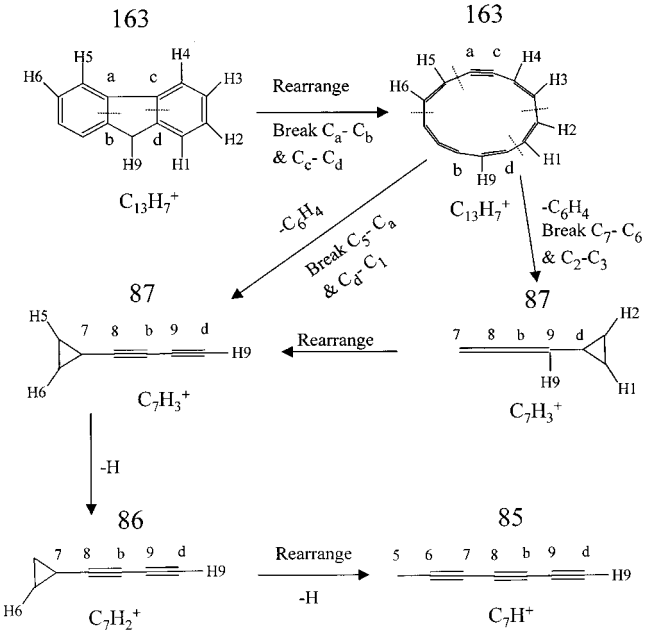

Figure 5. Formation of *m*/*z* 87 ($C_7H_3^+$) and *m*/*z* 85 (C_7H^+) ions from the *m*/*z* 163 isomer ($C_{13}H_7^+$ form d in Figure 2).

also produced the *m*/*z* 87 ($C_7H_3^+$), 86 ($C_7H_2^+$), and 85 (C_7H^+) ions. It is also known from experiment that both the *m*/*z* 163 and 161 precursors lead to *m*/*z* 85 and 63 products. One possibility is that different isomers of the precursors lead to different final products, with masses that just happen to be the same, i.e., either *m*/*z* 85 or 63.

ii. Photoproducts from the m/z 163 Ion. Photolysis of the *m*/*z* 163 ion produces *m*/*z* 162, 161, 89, and 87 product ions directly (cf. Figure 1). These products, which result from the ejection of H, H_2, C_6H_2, and C_6H_4 neutral fragments, are understandable if one assumes that the *m*/*z* 163 ion initially exists in four isomeric fluorene-like forms (cf. Figure 2, forms 163a−d). As an example, consider the *m*/*z* 163c and 163d isomers. The first has the H5, H8, and H9′ hydrogens removed (cf. Figure 3 and 4), while the second has the H7, H8, and H9′ hydrogens stripped (cf. Figure 5). The first may rearrange, by breaking its internal C_a-C_b and C_c-C_d bonds, to form a monocyclic ring which, upon absorption of more energy, may break its C_4-H_4 and C_1-H_1 bonds and form the *m*/*z* 161 $C_{13}H_5^+$ cyclic structure (cf. Figure 3).

The *m*/*z* 89 cation may be produced directly from the *m*/*z* 163c precursor (cf. Figure 4). The most stable form for this product ion is a six-membered ring, formed by ring closure of

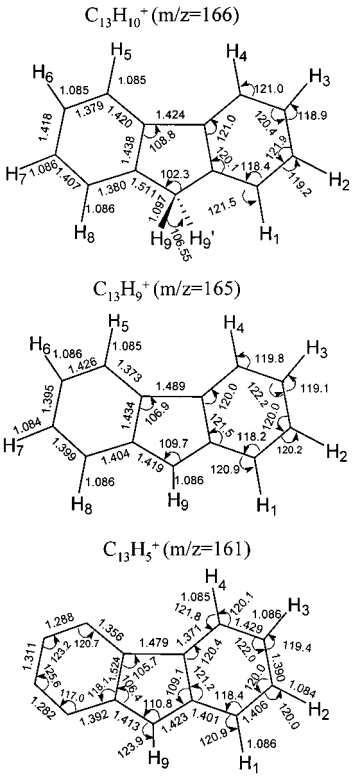

Figure 6. Optimized geometries for fluorene-like structures: fluorene cation, $C_{13}H_{10}^+$, *m*/*z* 166; fluorene cation fragment minus one hydrogen (H9′), $C_{13}H_9^+$, *m*/*z* 165; fluorene cation fragment minus five hydrogens (H9′, H8, H7, H6, and H5), $C_{13}H_5^+$, *m*/*z* 161; all at B3LYP/6-31G-(d,p) levels.

the C_c and C_d carbons, fused with a three-membered ring (cf. Figures 4). Figure 5 gives a possible photofragmentation scheme for the *m*/*z* 163d isomer. Since the placement of the hydrogens on the original fluorene-like framework is different in this isomer, it is now possible, after ring opening, to eject two different C_6H_4 neutral fragments without any hydrogen relocations. This may occur by breaking either the C_5-C_a, C_d-C_1 bond set or the C_6-C_7, C_2-C_3 bond set, both of which lead to a different *m*/*z* 87 ($C_7H_3^+$) ion. One of these may then rearrange to form the lower energy species having a "tadpole-like"shape (i.e., a three-membered ring attached to an acetylenic carbon chain tail).

iii. Photoproducts from the m/z 161 Ion. Photolysis of the *m*/*z* 161 ion produces the *m*/*z* 135, 111, 87, and 63 products directly (cf. Figure 1). Both the *m*/*z* 135 and 111 products lose three hydrogens sequentially to yield the *m*/*z* 132 and 108 species, respectively. The *m*/*z* 87 product loses two hydrogens to give the *m*/*z* 85 ion. This sequence is shown in Figure 3. The monocyclic ring form of the $C_{13}H_7^+$ (*m*/*z* 163) precursor initially loses two hydrogens (H1 and H4) to give $C_{13}H_5^+$ (*m*/*z*/161), which may then decompose in one of four ways, i.e., by ejecting one of the neutral fragments C_2H_2, C_4H_2, C_6H_2, or C_8H_2. Ejection of C_2H_2 leads to $C_{11}H_3^+$ (*m*/*z* 135) and, thence, with the elimination of three hydrogens, to C_{11}^+ (*m*/*z* 132). Ejection of C_4H_2 yields $C_9H_3^+$ (*m*/*z* 111) and finally, after the elimination of three hydrogens, C_9^+ (*m*/*z* 108). Removal of C_6H_2 from $C_{13}H_5^+$ leaves $C_7H_3^+$(*m*/*z* 87), which then further loses two hydrogens to give C_7H^+ (*m*/*z* 85). Stripping of C_8H_2 from $C_{13}H_5^+$ leaves the $C_5H_3^+$ (*m*/*z* 63) product.

The most stable geometries of the initial precursors (*m*/*z* 166, 165, and 161) and of the final photodecomposition products have been calculated and are shown in Figures 6 and 7,

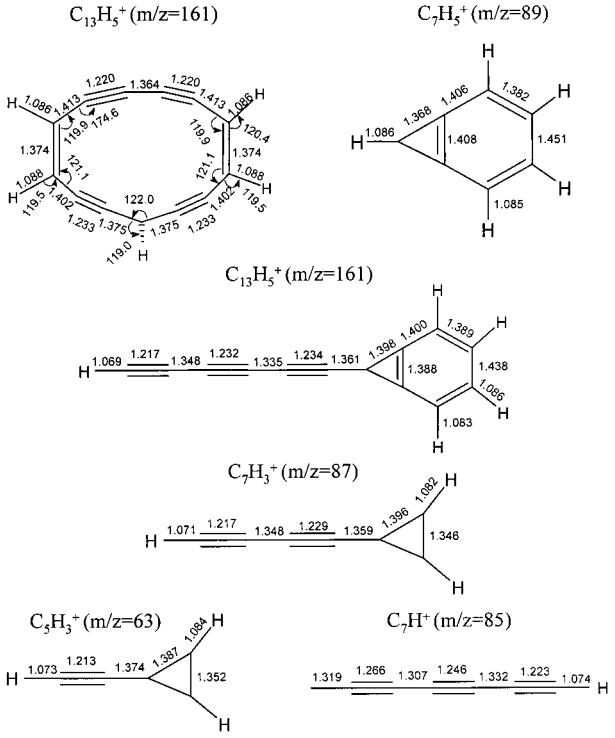

Figure 7. Optimized structures (B3LYP/6-31G(d,p)) for the *m*/*z* 63, 85, 87, 89, and two different *m*/*z* 161 cations, proposed as photolysis products of the fluorene cation. Bond lengths are in angstroms and angles in degrees. These are the lowest energy isomers found on the potential surface. The calculated energy (B3LYP/6-31G(d,p)) of the *m*/*z* 161 cyclic isomer is 0.698 eV above the chain−triangle−ring structure.

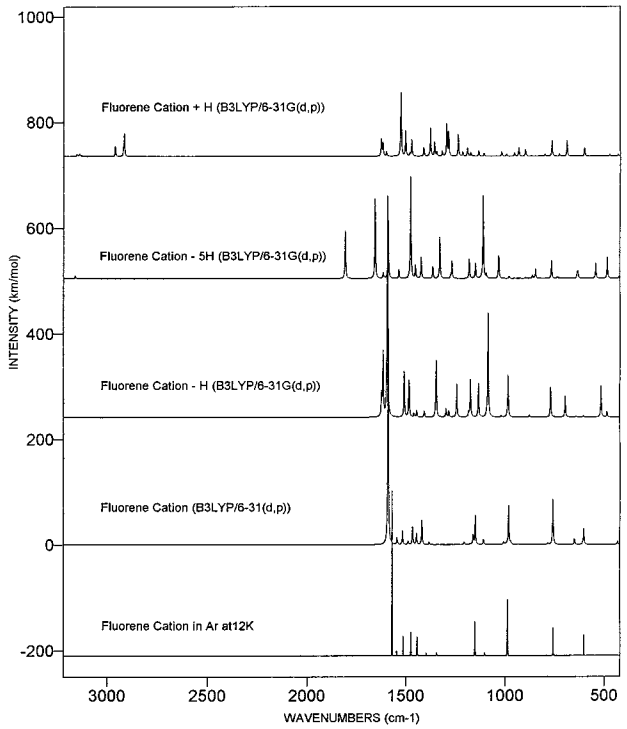

Figure 8. Infrared absorption spectra for fluorene cation $C_{13}H_{10}^+$, dehydrogenated fluorene cations $C_{13}H_9^+$ and $C_{13}H_5^+$, and the most stable hydrogenated fluorene cation $C_{13}H_{10}^+ + H6'$; B3LYP/6-31G(d,p) level (0.978 scale factor). The experimental absorption spectrum of the fluorene cation in solid Ar at 12 K (with relative band intensity) is displayed for comparison (adapted from ref 13). The close-lying 1572.4/1564.8 cm^{-1} doublet band (in Ar) is displayed as one band whose intensities have been added.

respectively. $C_5H_3^+$, like its larger cousin, $C_7H_3^+$, has a tadpole-like structure, while C_7H^+ prefers a linear acetylenic form with a hydrogen at one end. The pure carbon products, C_9^+ and C_{11}^+, have been studied previously by Giuffreda et al.[14] and Bowers and co-workers.[15,16] Different calculations (using B3LYP/cc-pVDZ, B3PW91/cc-pVDZ, and CCSD(T)) indicate that both these species are probably monocyclic. However, a linear structure for C_9^+ cannot excluded, since its energy lies only 1.7 kcal/mol (B3LYP) or 13.1 kcal/mol (CCSD(T)) above the monocyclic (C_{2v}, $^2B_1$) form.[14]

d. Infrared Spectra for Fluorene Cation and Its Dehydrogenated Products. Matrix isolation infrared spectroscopy could be used to confirm the final product structures proposed here, provided the sample is prepared under conditions that favor ion fragment formation.[17] While difficult, this approach has been used successfully in the past to obtain infrared spectra of PAH ions in the presence of parent neutrals. A key element of this approach is the availability of reliable predicted spectra of the expected products. Here we present the predicted IR spectra of the fluorene cation and two of its principal dehydrogenated products ($C_{13}H_9^+$, and $C_{13}H_5^+$).

The scheme proposed above for the dehydrogenation of the fluorene cation (to $C_{13}H_5^+$) assumed that, during the dehydrogenation steps, the carbon framework retains its fluorene-like skeleton and does not rearrange. Confirmation of this was sought from computed spectra and matrix isolation infrared (IR) experiments.[17] Figure 6 shows the optimized structures of the $C_{13}H_{10}^+$, $C_{13}H_9^+$, and $C_{13}H_5^+$ species for which IR spectra were computed, while Figure 8 shows the predicted and experimental spectra of the fluorene cation. Strong IR-active bands are predicted for $C_{13}H_5^+$ (using B3LYP/4-31G (B3LYP/6-31G (d,p))) at 1772 (1804), 1619 (1654), 1559 (1588), 1459 (1477), and 1099 (1111) cm^{-1} (scaling factor of 0.957 (0.978)). The first band is a C−C vibration centered predominantly in the dehydrogenated ring. As Figure 8 shows, calculated spectra of other fluorene species show no other bands in this region, for either hydrogenated or dehydrogenated fluorene ions. The observed spectrum for the fluorene cation (cf. bottom panel, Figure 8) shows no bands in this region. But when the experimental conditions are optimized for the production of fragments of the fluorene cation during matrix deposition, a set of bands appears at 1742.4, 1553.8, 1442.0, and 1085.8 cm^{-1}. These bands are in good agreement with the calculated positions. The calculated 1619 (1654) cm^{-1} band lies in the water O−H bending region. No fragment band was found in this region. This result lends strong support to the assumption above that fluorene, devoid of five hydrogens, retains its fluorene-like framework after dehydrogenation *and* that the five hydrogens are removed from only one of the six-membered rings.

Several interesting features of the predicted spectra can be noted. First, the experimental spectrum of the fluorene cation (Ar, 12 K), here reproduced with stick figure bands for ease of comparison, matches the predicted spectrum very well. Bands are neither predicted nor observed in the CH stretching range. The most intense observed band doublet at 1564.8/1572.4 cm^{-1} (shown as a single peak) is predicted to lie at 1587.5 cm^{-1}, showing only a slight shift between theoretical and experimental values. And, the frequency distribution of the other bands is generally excellent even though only one scaling factor was applied. Second, the singly dehydrogenated fragment shows two intense bands in the region where only one was seen in the cation and its bands in the 1000−1500 cm^{-1} region are stronger and more numerous. Third, computation of the IR of the

TABLE 2: C−H Bond Energies (eV, ZPE × 0.957 Corrected) of Hydrogenated Fluorene Cations $C_{13}H_{11}^+$ (*m*/*z* 167) and $C_{13}H_{12}^+$ (*m*/*z* 168) (B3LYP/4-31G Level)

	H added							
precursor label	H1′	H2′	H3′	H4′	H5′	H6′	H7′	H8′
	First H Added (*m*/*z* 166 → 167)							
(166)	2.35	2.21	**2.74**	2.64	2.64	**2.74**	2.21	2.35
	Second H Added (*m*/*z* 167 → 168)							
H6′ + (166)	1.05	1.05	0.71	1.01	**2.06**		1.53	1.87

[a] The position of hydrogens added in $C_{13}H_{10}^+$ and $C_{13}H_{11}^+$ is given in Figure 2. The most exothermic reactions are given in bold type.

fragment species with five missing hydrogens displays bands that are close to the observed bands. This match shows the power of the combined matrix isolation infrared spectroscopic and DFT theory computational approaches as a diagnostic for the identification of the fragment species.

e. Reaction of Fluorene Cation with Hydrogens. It has been proposed that hydrogenation reactions of the PAH cations may be important astrochemically.[7,12] Calculations were performed here on the addition of one or two hydrogens to the fluorene cation. The calculated CH bond energies are given in Table 2.

i. Addition of First Hydrogen. All hydrogenation reactions with the fluorene cation are computed to be exothermic. The strongest CH bond, at the H6′ position (and equivalent H3′ position), has an energy of 2.74 eV (63.3 kcal/mol). The infrared absorption spectrum calculated for the $C_{13}H_{11}^+$ ion is displayed in Figure 8. The comparison of this spectrum with the one for the fluorene cation reveals additional bands in the CH stretching region. Reasonably strong bands at 2957 cm^{-1} (31 km/mol), 2915 cm^{-1} (13 km/mol), and 2912 cm^{-1} (41 km/mol) are predicted. The former band is a vibration involving the H9 and H9′ atoms, whereas the latter two (actually a doublet) are antisymmetric stretching vibrations of the CH6 and CH6′ bonds. In general, CH vibrations in $C_{13}H_{11}^+$ are more intense than in the parent ion. The intensity distribution in the CC stretching range is different than in the parent cation and, in the 1000−1200 cm^{-1} region, the bands are predicted to be much weaker than in the parent cation.

We note that the hydrogenation of the naphthalene cation was examined by Bauschlicher who found that the addition of a single hydrogen was exothermic by ca. 62 kcal/mol.[12] This is consistent with the observations of Bierbaum and Snow and co-workers.[7]

ii. Addition of Second Hydrogen. Addition of the second hydrogen to the fluorene cation is also exothermic, but somewhat less so. The strongest CH bond energies are 2.06 eV (54.2 kcal/mol) when a hydrogen is added at position H5′ in $C_{13}H_{11}^+$ (first hydrogen at H6′); cf. Table 2. Adding the second hydrogen to the *other* six-membered ring results in 50% smaller bond energies.

Infrared spectra were also generated for doubly hydrogenated fluorene ions. As found for the singly hydrogenated system, the IR band intensities in the CH stretching region are predicted to be substantially more intense than in the parent cation. This observation is true for all hydrogenated fluorene species studied here.

iii. Loss of Hydrogens from Hydrogenated Fluorene Cations. Another class of reaction considered here is the abstraction of hydrogen atoms (particularly H9 or H9′) from $C_{13}H_{11}^+$ (or $C_{13}H_{12}^+$) triggered by incoming atomic hydrogen, and resulting in the products H_2 and $C_{13}H_{10}^+$ (or $C_{13}H_{11}^+$). This reaction was considered earlier by Bauschlicher for the 1-hydronaphthalene cation for which a very small (0.25 kcal/mol) barrier was predicted.[12] Bauschlicher reported that the energy barrier for this type of reaction decreases with increasing PAH size. Thus, for the fluorene cation, it is expected that there should be a very low (or no) barrier to the abstraction reaction. Indeed, because the H−H bond energy (calculated as 103.67 kcal/mol) is so much higher than the CH bond energy (63.25 kcal/mol) for two hydrogens bonded to the same carbon, it is clear that the formation of H_2 from hydrogenated fluorene cations could be a very efficient process.

IV. Conclusions

In an earlier experimental paper, evidence from an FTICR/MS study was presented on the photodecomposition of gaseous fluorene cations. The primary decomposition pathway was found to be the sequential loss of five hydrogen atoms and, with additional irradiation, the further decomposition of these dehydrogenated products to lower mass fragments. In this paper, the results of density functional theory calculations (mainly B3LYP/4-31G level) are presented. It is shown that the most probable positions for extraction of the five hydrogens are, first, from the sp^3 carbon and, subsequently, from the four positions on one of the six-membered rings. Removal of hydrogens on the other ring and removal of a sixth hydrogen requires substantially higher energies.

Further fragmentation of the odd mass dehydrogenated products (*m*/*z* 165, 163, and 161) has been explored theoretically and various monocyclic ring intermediates have been suggested, which lead plausibly to the observed lower mass final products. Unusual geometries are proposed for some of the products, such as a cyclopropyl ring fused to a six-membered ring for the $C_7H_5^+$ product, a "tadpole" shape (three-membered ring attached to a linear carbon chain) for the $C_5H_3^+$ species, and monocyclic rings for the all-carbon C_9^+ and C_{11}^+ product ions.

Infrared spectra have also been calculated for the fluorene cation, and hydrogenated and dehydrogenated products. Spectral differences, which may aid in the determination of the species produced, have been noted. The appearance of matrix IR bands at 1742.4, 1553.8, 1442, and 1085.5 cm^{-1} generated during deposition under conditions optimized for fluorene cation fragment production is taken as evidence for the fluorene cation with five of its hydrogens removed and retention of the fluorene-like framework.

Experimental evidence for the structures of the proposed species is certainly of great interest, not only for the specific case of fluorene, but also for other PAHs. If it were possible to demonstrate that the proposed geometries are correct, it would lend credence to the approach used here (i.e., the use of DFT theory on ground electronic states to predict structures of species that are generated photochemically) and show that PAHs or PAH-like cationic species can be photodecomposed to all-carbon chains or rings. It would also provide strong, though indirect, evidence that fluorene (and other PAHs?) readily rearrange to intermediate structures such as monocyclic rings. Efforts are underway to combine a FTICR mass spectrometer with a continuously tunable infrared source to perform these experiments.

Acknowledgment. We acknowledge the National Aeronautics and Space Administration and the Petroleum Research Foundation, administered by the American Chemical Society, for their support of this research, and the Northeast Regional Data Center for a grant under the Research Computing Initiative for computer time.

References and Notes

(1) Siegmann, K.; Sattler, K. *J. Chem. Phys*. **2000**, *112*, 698 and references therein.

(2) Leger, A.; Puget, J. L. *Astron. and Astrophys*. **1984**, *137*, L5.

(3) Allamandola, L. J.; Tielens, A. G. G. M.; Barker, J. R. *Astrophys. J*. **1985**, *290*, L25.

(4) Russel, R.; Soifer, B.; Willner, W. *Astrophys. J*. **1977**, *217*, L149; **1987**, *220*, 568.

(5) Szczepanski, J.; Vala, M. *Nature* **1993**, *363*, 699.

(6) Joblin, C.; Tielens, A. G. G. M.; Geballe, T. R.; Wooden, D. H. *Astrophys. J*. **1996**, *460*, L119−L122.

(7) Snow, T. P.; Page, V. L.; Keheyan, Y.; Bierbaum, V. *Nature* **1998**, *391*, 259.

(8) Ekern, S. P.; Marshall, A. G.; Szczepanski, J.; Vala, M. *Astrophys. J*. **1997**, *L39*−*L41*, 488.

(9) Ekern, S. P.; Marshall, A. G.; Szczepanski, J.; Vala, M. *J. Phys. Chem*. **1998**, *102*, 3498.

(10) Dibben, M. J.; Kage, D.; Szczepanski, J.; Eyler, J. R.; Vala, M. *J. Phys. Chem.* **2001**, *105*, 6024.

(11) Frisch, M. J.; Trucks, G. W.; Schlegel, H. B.; Scuseria, G. E.; Robb, M. A.; Cheeseman, J. R.; Zakrzewski, V. G.; Montgomery, J. A., Jr.; Stratmann, R. E.; Burant, J. C.; Dapprich, S.; Millam, J. M.; Daniels, A. D.; Kudin, K. N.; Strain, M. C.; Farkas, O.; Tomasi, J.; Barone, V.; Cossi, M.; Cammi, R.; Mennucci, B.; Pomelli, C.; Adamo, C.; Clifford, S.; Ochterski, J.; Petersson, G. A.; Ayala, P. Y.; Cui, Q.; Morokuma, K.; Malick, D. K.; Rabuck, A. D.; Raghavachari, K.; Foresman, J. B.; Cioslowski, J.; Ortiz, J. V.; Stefanov, B. B.; Liu, G.; Liashenko, A.; Piskorz, P.; Komaromi, I.; Gomperts, R.; Martin, R. L.; Fox, D. J.; Keith, T.; Al-Laham, M. A.; Peng, C. Y.; Nanayakkara, A.; Gonzalez, C.; Challacombe, M.; Gill, P. M. W.; Johnson, B.; Chen, W.; Wong, M. W.; Andres, J. L.; Gonzalez, C.; Head-Gordon, M.; Replogle, E. S.; Pople, J. A. *Gaussian 98*, Revision A.3; Gaussian, Inc.: Pittsburgh, PA, 1998.

(12) Bauschlicher, C. W., Jr. *Astrophys. J*. **1998**, *509*, L125−L127 and references therein.

(13) Langhoff, S. R. *J. Phys. Chem*. **1996**, *100*, 2819.

(14) Giuffreda, M. G.; Deleuze, M. S.; Francois, J. P. *J. Phys. Chem. A* **1999**, *103*, 5137.

(15) von Helden, G.; Hsu, M. T.; Kemper, P. R.; Bowers, M. T. *J. Chem. Phys*. **1991**, *95*, 3835.

(16) von Helden, G.; Gotts, N. G.; Bowers, M. T. *J. Am. Chem. Soc*. **1993**, *115*, 4363.

(17) Szczepanski, J.; Banisaukas, T. J.; Vala, M.; Hirata, S.; Bartlett, R. J.; Head-Gordon, M. *J. Phys. Chem*., submitted.